Title

Reaction amplification with a gain: Triplet exciton-mediated quantum chain using mixed crystals with a tailor-made triplet sensitizer.

Journal

Proceedings of the National Academy of Sciences, 121(14)

Authors

Paul, Indrajit
Konieczny, Krzysztof
Chavez, Roberto
et al.

Publication Date

2024-04-02

DOI

10.1073/pnas.2401982121

Peer reviewed

PNAS INAUGURAL ARTICLE | CHEMISTRY

Reaction amplification with a gain: Triplet exciton–mediated quantum chain using mixed crystals with a tailor-made triplet sensitizer

Indrajit Paul[a], Krzysztof A. Konieczny[a], Roberto Chavez[a], and Miguel A. Garcia-Garibay[a,1]

This contribution is part of the special series of Inaugural Articles by members of the National Academy of Sciences elected in 2023.
Contributed by Miguel A. Garcia-Garibay; received January 29, 2024; accepted February 26, 2024; reviewed by Michael R. Wasielewski and V. Ramamurthy

Photochemical valence bond isomerization of a crystalline Dewar benzene (DB) diacid monoanion salt with an acetophenone-linked piperazinium cation that serves as an intramolecular triplet energy sensitizer (DB-AcPh-Pz) exhibits a quantum chain reaction with as many as 450 product molecules per photon absorbed ($\Phi \approx 450$). By contrast, isomorphous crystals of the DB diacid monosalt of an ethylbenzene-linked piperazinium (DB-EtPh-Pz) lacking a triplet sensitizer showed a less impressive quantum yield of ca. $\Phi \approx 22$. To establish the critical importance of a triplet excited state carrier in the adiabatic photochemical reaction we prepared mixed crystals with DB-AcPh-Pz as a dilute triplet sensitizer guest in crystals of DB-EtPh-Pz. As expected from their high structural similarities, solid solutions were easily formed with the triplet sensitizer salt in the range of 0.1 to 10%. Experiments carried out under conditions where light is absorbed by the triplet sensitizer-linked DB-AcPh-Pz can be used to initiate a triplet state adiabatic reaction from ^{3}DB-AcPh-Pz to ^{3}HB*-AcPh-Pz, which can serve as a chain carrier and transfer energy to an unreacted DB-EtPh-Pz where exciton delocalization in the crystalline solid solution can help carry out an efficient energy transfer and enable a quantum chain employing the photoproduct as a triplet chain carrier. Excitation of mixed crystals with as little as 0.1% triplet sensitizer resulted in an extraordinarily high quantum yield $\Phi \approx 517$.

mixed crystals | exciton-enabled | triplet excited state | quantum chain reaction | solid-state reaction

Significance

Crystalline materials designed for the chemical amplification of photons with a significant gain have a potential for enabling optical, sensing, imaging, and energy transduction applications with highly enhanced sensitivity. To that end, we have used the adiabatic valence-bond isomerization of a Dewar benzene (**DB**) to its corresponding Hückel benzene isomer in mixed crystals grown with a tailor-made sensitizer to establish that a triplet exciton carrier leads to quantum chain reactions where every photon results in up to 517 product molecules, with as little as 0.1% of the triplet sensitizer. Mixed crystals designed for this study are based on the use of isomorphous ionic auxiliaries both as crystal engineering handles and as triplet sensitizers.

Most photochemical and photophysical processes in dilute solution and in the gas phase occur by the absorption of one photon per event, as opportunities for strong coupling between ground and excited state molecules are limited by brief and infrequent encounters. In contrast, strong coupling in crystals creates opportunities for the generation of more than one excited state per photon in the form of exciton fission (1, 2), or the fusion of excited states leading to the formation of higher excited state by combining the energy of two low energy photons (3, 4). Another promising but significantly less studied process occurs when a single photon results in many chemical events by exciton-mediated energy transfer in quantum chain reactions (Fig. 1) (5, 6).

The number of quantum chain reactions reported in the literature is relatively small. Examples include cis-trans isomerization of alkenes and polyenes (7–9) dissociation of dioxetanes to ground and excited state ketones (10, 11). and some bond-valence isomerizations (12). These reactions rely on excited states that undergo adiabatic reactions where the products are formed in the same excited state as the reactant, as shown in Fig. 1*A* ($R_1^* \rightarrow P_1^*$). When generated in crystals, efficient electronic coupling between close neighbors (Fig. 1*B*) results in rapid exciton delocalization and energy transfer from an excited photoproduct to new ground state reactant, $P_1^* + R_2 \rightarrow P_1 + R_2^*$, which creates an opportunity to propagate a quantum chain. As indicated in Fig. 1*C*, the quantum chain is initiated by generation of the excited reactant, either by direct absorption of a photon, or by energy transfer from a competent sensitizer [step (1)]. Efficient propagation requires adiabatic reactions [step (2)] with rates k_{AR} that are much greater than the rate of decay of the excited reactant, k_{RD} in step (4), so that the quantum yield per step approaches unity [$\Phi_{AR} = k_{AR}/(k_{AR} + k_{RD}) \approx 1$]. In a similar manner, the rate of excitation transfer from product to reactant in step (3) must be greater than the rate of decay of the excited photoproduct in step (4'). Given that exciton delocalization and energy transfer in crystals are generally very fast, adiabatic reactions with high quantum yields ($\Phi_{AR} \approx 1$) should have a number of steps in the chain (n) that is limited by the lifetime of the excited photoproduct.

Author affiliations: [a]Department of Chemistry and Biochemistry, University of California, Los Angeles, CA 90024-1569

Author contributions: I.P. and M.A.G.-G. designed research; I.P., K.A.K., R.C., and M.A.G.-G. performed research; M.A.G.-G. analyzed data; and I.P. and M.A.G.-G. wrote the paper.

Reviewers: M.R.W., Northwestern University; and V.R., University of Miami.

The authors declare no competing interest.

[1]To whom correspondence may be addressed. Email: mgg@chem.ucla.edu.

This article contains supporting information online at https://www.pnas.org/lookup/suppl/doi:10.1073/pnas.2401982121/-/DCSupplemental.

Published March 27, 2024.

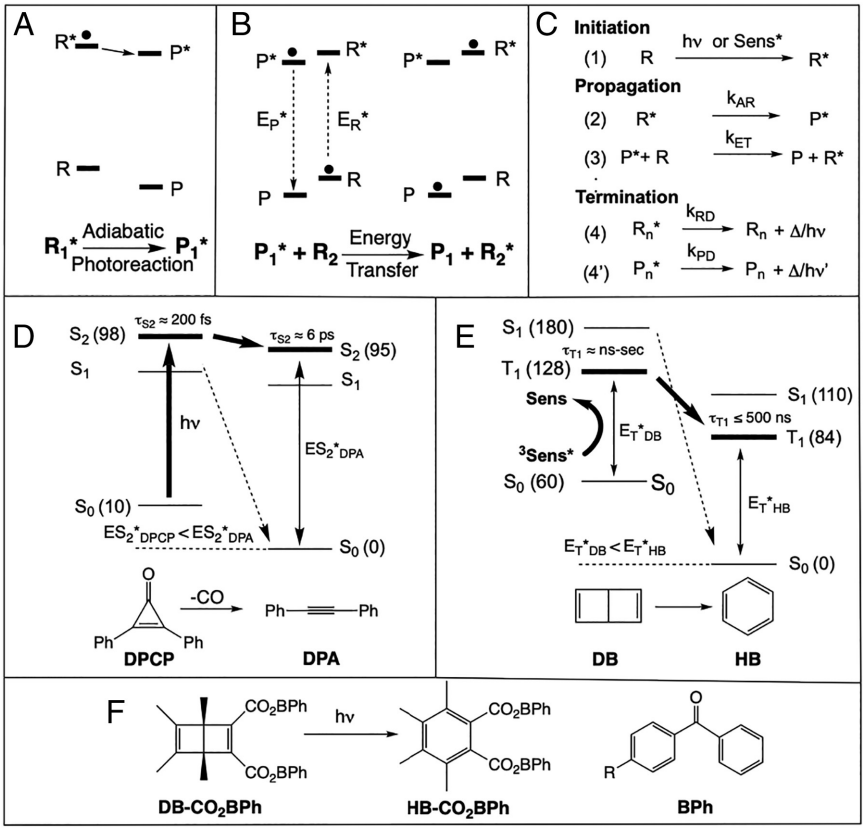

Fig. 1. A quantum chain reaction relies on (*A*) an adiabatic photochemical reaction followed by (*B*) unidirectional energy transfer from the excited photoproduct to a new reactant molecule. (*C*) Initiation, propagation and termination steps involved in a quantum chain reaction. Energy diagrams for the adiabatic reactions of (*D*) **DPCP** to **DPA** along the second single excited state surface (S_2), and (*E*) Dewar (**DB**) to **HB** along the lowest triplet excited state (T_1). Normal nonadiabatic reactions from S_1 to S_0 in both cases are shown with dotted arrows. Relative energies reported in the literature are given in parenthesis in kcal/mol along with excited state lifetimes previously reported in solution at 295 K. Lifetimes of triplet benzene in solution are strongly concentration-dependent. (*F*) Quantum chain reaction of intramolecularly triplet-sensitized crystalline bis-(4-hydroxybenzophenone)-tetramethyl-dewar-benzene-1,2-dicarboxylate (**DB-CO_2BPh**).

The key role of exciton delocalization on the efficiency of a quantum chain reaction, and the limiting effect of the excited product lifetime were highlighted with the reaction of crystalline diphenylcyclopropenone (**DPCP**) to crystalline diphenyl acetylene (**DPA**, Fig. 1*D*) (9, 10). Previous reports carried out in solution had suggested an adiabatic reaction with a time constant of only 200 fs from the second excited state of the reactant to the second excited state of the photoproduct (13) and indicated that the S_2 of **DPA** only lasted for ca. 6 ps before starting a decay into the ground state photoproduct. Using nanocrystalline suspensions to carry out quantum yield determinations (14) and femtosecond pump–probe spectroscopy (15) we confirmed a quantum chain with an average of 3.3 product molecules per photon absorbed (4), indicating that energy transfer in crystals occurred with an average time constant of 1.8 ps per step.

With efficient energy transfer by fast exciton delocalization, adiabatic reactions along long-lived triplet surfaces should undergo quantum chain reactions with many more product molecules per photon.* Looking for a suitable test system to test this hypothesis, we recognized that the photochemical valence bond isomerization of triplet Dewar benzene (**DB**) to Huckel benzene (**HB**) (benzene henceforth) meets the desired criteria (12, 16). As shown in Fig. 1*E*, while triplet **DB** has a relatively high triplet energy of 68 kcal/mol, it is significantly lower than the one of benzene, at 84 kcal/mol, such that energy transfer in a quantum chain reaction should be highly exothermic and favorable. The triplet lifetime of **DB** is not known but it is limited by the time constant of its adiabatic reaction, which has a quantum yield $\Phi_{AR} \approx 1$ (12). By contrast, the triplet lifetime of benzene is concentration-dependent and varies from a few nanoseconds to a few hundred nanoseconds in solution at ambient temperature (17), and it extends into a few seconds in dilute matrices at cryogenic temperatures and in crystals (18). Early studies with **DB** in solution showed concentration-dependent quantum yields as high as ca. 120 (19) consistent with a quantum chain reaction that is limited by diffusion-mediated energy transfer.

In order to carry out a triplet-sensitized photochemical reaction in the crystalline state we recently explored the solid-state photochemistry of tetramethyl-**DB**-1,2-dicarboxylate equipped with two 4-hydroxy-benzophenones (**DB-CO_2BPh**, Fig. 1*F*) (19, 20). The solid-state reaction occurred with high chemical efficiency and quantum yields up to ca. Φ = 300 with polycrystalline powders suspended in a dilute surfactant. However, we were not able to detect the triplet carrier ^{3}**HB-CO_2Ph*** in the solid state, suggesting that the quantum chain reaction may be limited by a lifetime that is shorter than the 10 ns laser pulse width (20).

Recognizing that crystalline benzophenones are prone to reductive self-quenching, we designed a reaction system based on mixed crystals where the concentration of a tailor-made triplet sensitizer can be varied over a wide concentration range (21–24) Considering that formation of mixed crystals with random occupancies generally requires components with a coefficient of structural similarity greater than 85%, we recognized that the structure of the reactant and the triplet sensitizer must be very similar. The design reported in this paper is based on a modular approach based on

*If one assumes an efficient adiabatic reaction, exciton energy transfer rates of $k_{ET} = 10^{12}$ steps per second, and triplet lifetimes in the microsecond regime ($\tau_T = 10^{-6}$ s), one would expect an upper limit of $n = k_{ET} * \tau_T = 10^6$ product molecules per photon.

the use of an ionic crystal engineering auxiliary (25) to modify readily available tetramethyl Dewar benzene diacid (**DBDA**) (Fig. 2*A*). Looking for two similar amines that could act as a triplet sensitizer and crystal engineering handles, respectively, we explored the use of 4-acetylphenyl-piperazine **AcPh-Pz** and 4-ethylphenyl-piperazine **EtPh-Pz**, which differ only by having a carbonyl in the triplet sensitizer and a CH_2 in the ionic auxiliary. The structures of the quantum chain crystal host reactant and its tailor-made triplet sensitizer guest are illustrated in Fig. 2*A*.

Application of the quantum chain mechanism in Fig. 1*C* to mixed crystals of **DB** piperazinium monocarboxylates in Fig. 2*A*, is expected to start with excitation and intersystem crossing (isc) of the acetophenone chromophore in **DB–AcPh-Pz** followed by intramolecular triplet energy transfer to the **DB** chromophore that initiates the quantum chain (Fig. 2*B*). The propagation steps involve a triplet state adiabatic reaction from **DB** to benzene (Fig. 2*C*, X=CO), followed by triplet energy transfer from triplet benzene to an unreacted **DB** of the more abundant ethyl-benzene piperazinium salt (Fig. 2*D*). Chain propagation proceeds by iteration of equations C and D, with the more abundant ethyl-phenyl piperazinium salt **HB-EtPh-Pz** acting as the main quantum chain carrier.

In this paper, we describe the synthesis of the components introduced in Fig. 2, the crystallization and structural characterization of crystals of the pure components and mixed crystalline specimens, and results from a quantum chain reaction studied in reverse-phase nanocrystalline suspensions using hexane as the supporting solvent. Key results include the spectroscopic and kinetic characterization of the triplet benzene quantum chain carrier, ^{3}**HB*–EtPh-Pz**, and a quantum yield of F_{CR} = 517 when the mixed crystal loading of the triplet sensitizer is as low as 0.1%.

Results and Discussion

Synthesis and Characterization of Host and Guest DBs. Dewar benzene diacid **(DBDA)** was obtained by hydrolysis of the corresponding dimethyl ester, which was itself prepared by $AlCl_3$-catalyzed reaction of 2-butyne and dimethyl acetylene dicarboxylate, as reported in the literature (26). The detailed procedure and the corresponding analytical data are described in supplementary information appendix. To prepare the ketone-containing crystal **DB-AcPh-Pz** (Fig. 2*A*) we combined **DBDA** and the piperazine-substituted acetophenone **AcPh-Pz** in a 1:1 molar ratio. Good quality single crystal plates were obtained by slow evaporation from a 1:3:3 mixture of MeOH, $CHCl_3$, and hexane at 298 K. Similarly, good quality needles were obtained for **DB-EtPh-Pz** using the same stoichiometry of **EtPh-Pz** and **DBDA** and in the same solvent system. Optical microscope images are included in *SI Appendix*, Figs. S2 and S3 of the *ESI* section. Melting in both cases occurred with simultaneous isomerization to the benzene products, **HB-AcPh-Pz** and **HB-EtPh-Pz**, at ca. 195 °C and 182 °C, respectively. Differential scanning calorimetric data are included in *SI Appendix*, Fig. S49.

Single Crystal X-ray Diffraction Analysis. Diffraction data from crystals of **DB-EtPh-Pz** and **DB-AcPh-Pz** were acquired at 100 K. They both belong to C2/c space group with one ion pair in

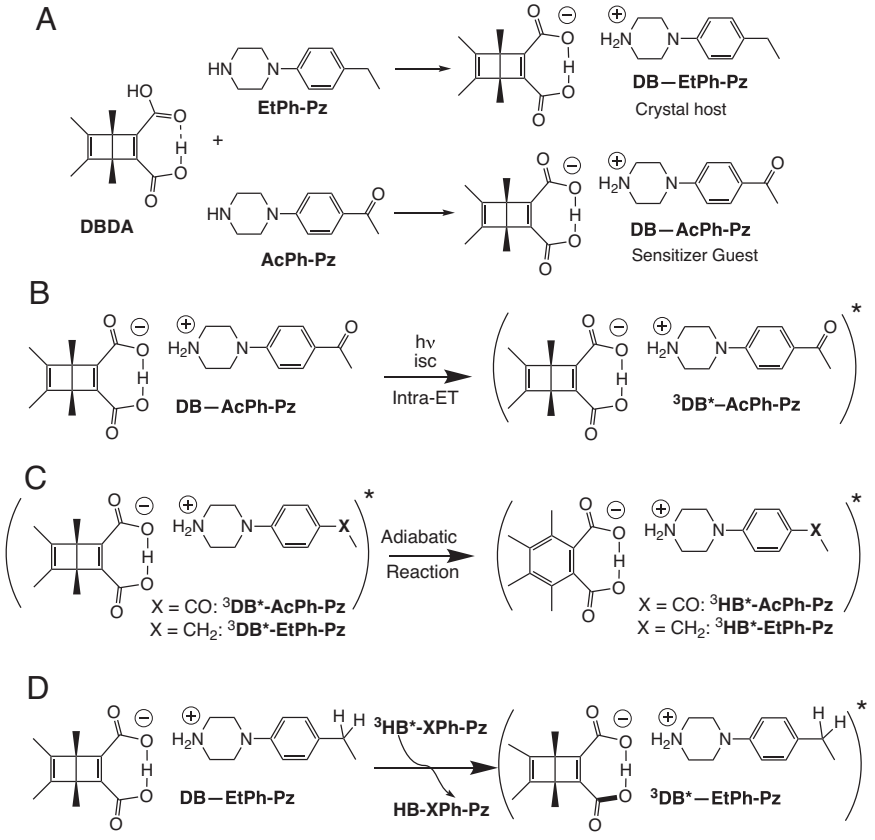

Fig. 2. (*A*) Preparation of **DB** dicarboxylates monosalts of acetophenone-linked piperazinium (**DB-AcPh-Pz**) and ethylbenzene-linked piperazinium cation (**DB-EtPh-Pz**). (*B*) Triplet **DB** generation by excitation and intersystem crossing of the acetophenone moiety followed by intramolecular energy transfer. (*C*) Adiabatic reaction from triplet **DB** to triplet benzene. (*D*) Intermolecular energy transfer from X=CO (^{3}**HB*-AcPh-Pz**) or X=CH_2 (^{3}**HB*-EtPh-Pz**). The overall quantum chain includes light excitation and intramolecular sensitization (*A*) followed by iteration of steps (*C*) → (*D*) → (*C*) → (*D*) → (*C*) → (*D*). Termination occur by excited state decay of the ^{3}**HB*-EtPh-Pz** chain carrier (not shown).

the asymmetric unit. As expected, the two ion pair structures are almost identical, as illustrated by their excellent overlap in Fig. 3*A*. Ion pairs are characterized by proton transfer from the **DB** diacid to the nitrogen atoms of the basic piperazines accompanied by the formation of strong intramolecular O-H···O hydrogen bonds (*SI Appendix*, Fig. S94). Both structures display orientational disorder. While the **DB** of **DB-AcPh-Pz** switches its concave face ca. 10% of the times, the phenylene ring of **DB-EtPh-Pz** adopts a slightly different torsional angle with 17.3% occupancy The basic supramolecular unit in the two crystals consist of tetrameric, cyclic hydrogen-bonding complexes with alternating **DB** monocarboxylates acting as hydrogen-bond acceptors, and the protonated piperazines acting as the hydrogen-bond donors (Fig. 3*A*). On a higher level of organization (Fig. 3 *C* and *D*), the orientation of the tetramers relative to each other is significantly different for the two crystals. The distribution of cations and anions for the CO-containing **DB-AcPh-Pz** forms chessboard-like motif (Fig. 3*C*) and those in the CH_2-containing **DB-EtPh-Pz** occur in fully separated layers of alternating cations and anions (Fig. 3*D*). A close inspection of the packing interaction near the CH_2 and CO groups of each crystal suggests that these packing differences may be determined by distinct C-H···O hydrogen bonding interactions.

Product Analysis in Solution and in Pure Crystals. We confirmed that the compounds designed for this study display the expected chemical reactivity summarized in Fig. 2 *B*–*D*. UV light exposure (l > 340 nm) of the Dewar benzene diacid **DBDA**, the monoacid salt of the acetophenone piperazinium salt **DB-AcPh-Pz**, and the monoacid salt of ethylbenzene piperazinium salt **DB-EtPh-Pz** in 5 mM degassed DMSO-d_6 resulted in clean and complete conversion into the respective benzenes, **HBDA**, **HB-AcPh-Pz**, and **HB-EtPh-Pz**. The as-formed products and their separate components were characterized by conventional analytical methods, including ^{1}H NMR,^{13}C NMR, mass spectrometry, and ^{13}C CP/MAS (*SI Appendix*, Figs. S16–S21). Experiments with dry powders held between Pyrex glass slides revealed the formation of the same photoproducts as in solution, demonstrating a clean solid-to-solid reaction. Furthermore, nanocrystalline samples (see below) of **DB-AcPh-Pz** suspended in hexanes demonstrated remarkably high conversion within a few minutes whereas suspensions of **DB-EtPh-Pz** showed moderate conversion to the corresponding photoproduct. Powder X-ray diffraction analysis of reacted filtered samples showed a new set of peaks, indicating that reactions occur by a solid-to-solid reconstructive phase transition (*SI Appendix*, Fig. S53). Recrystallized samples of benzene photoproducts, **HB-AcPh-Pz** and **HB-EtPh-Pz**, were found to melt with decomposition at 195 °C and 185 °C, respectively. Unfortunately, samples of the recrystallized products were not suitable for structural elucidation by single crystal X-ray diffraction.

Preparation and Characterization of Mixed Crystals for Quantum Chain Reaction. The preparation of mixed crystals of the **DB-EtPh-Pz** host with ketone-containing **DB-AcPh-Pz** guest was explored by slow evaporation of MeOH, $CHCl_3$, and hexane (1:3:3) solutions with varying amounts of the two components. Solution samples containing between 0.1% and 20% of the ketone-containing **DB** were allowed to crystallize and their composition analyzed by ^{1}H NMR after dissolution. The results displayed in Fig. 3*B* reveal an equilibrium isotherm with close to linear incorporation of the guest

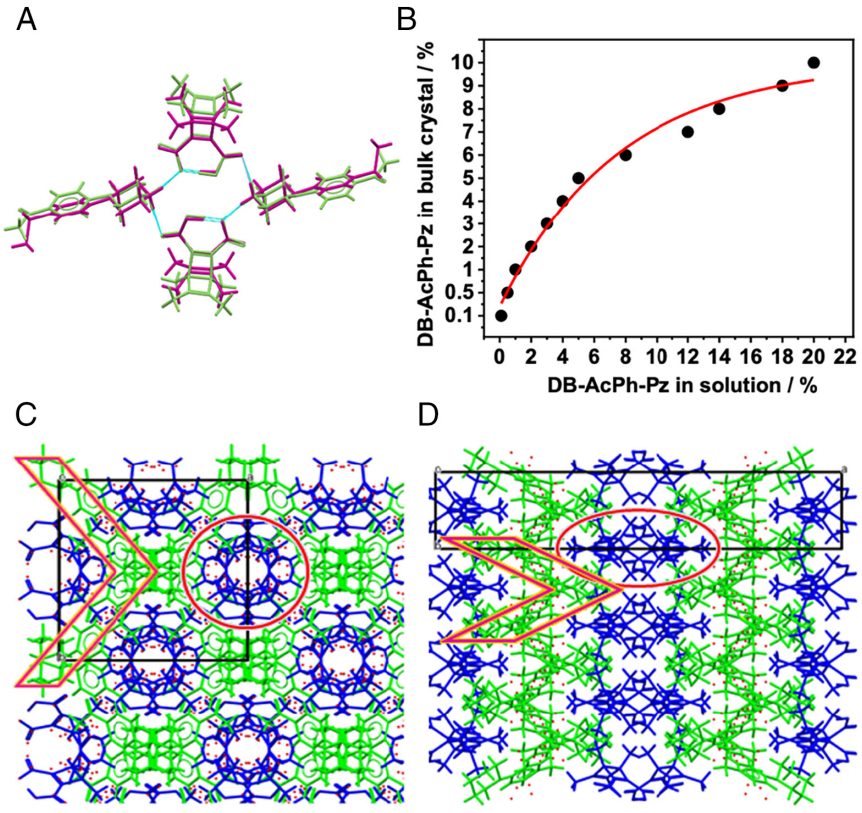

Fig. 3. (*A*) The cap stick depiction of overlapping X-ray molecular structures of **DB-AcPh-Pz** (magenta) and **DB-AcPh-Pz** (green) highlights the structural similarities of the molecular and supramolecular components. (*B*) Equilibrium isotherm of the incorporation **DB-AcPh-Pz** with concentration between 0% and 20% from mixed solvent system MeOH:$CHCl_3$: Hexane = 1:3:3. Crystal packing views of (*C*) **DB-AcPh-Pz** and (*D*) **DB-EtPh-Pz** in (001) plane. The **DB** anions and piperazinium cations are colored blue and green, respectively. The orientation of the two components are highlighted in red. The small red dots represent minor components of disordered fragments.

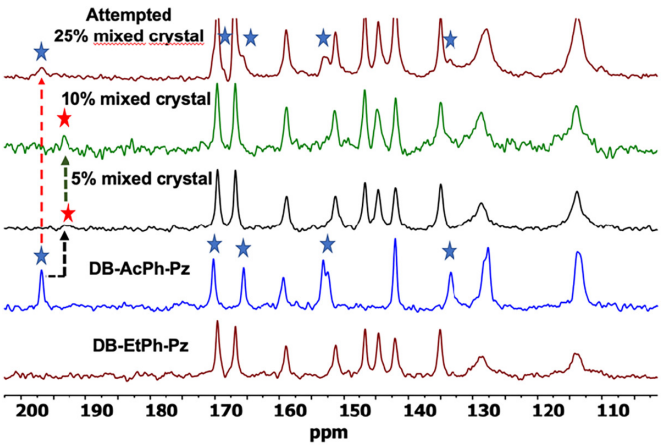

Fig. 4. Comparison partial solid-state ^{13}C CP/MAS NMR spectra (150 MHz, 298 K), from *Bottom* to *Top* of pure **DB-EtPh-Pz**, pure **DB-AcPh-Pz**, 5% mixed crystal **DB-AcPh-Pz**: **DB-EtPh-Pz** = 5:95, 10% mixed crystal **DB-AcPh-Pz**: **DB-EtPh-Pz** = 10:90, and attempt to obtain a higher concentration using 25% **DB-AcPh-Pz**. (peaks with blue asterisks corresponds to free **DB-AcPh-Pz** and peaks marked with the red asterisks to **DB-AcPh-Pz** in the mixed crystal).

up to ca. 5%, followed by saturation up to ca. 10%. The amount of ketone incorporated attained a maximum at ca. 8% and 10%, respectively, when solution concentrations were 14% and 20%. Attempts to grow mixed crystals with higher ketone concentration led to phase separation. A distinction between mixed crystals in the form of the desired substitutional solid solution instead of microphase segregation is consistent with the different packing arrangements of the segregated forms (Fig. 3 *C* and *D*). Furthermore, the formation of crystal domains was established by a combination of solid-state ^{13}C CP/MAS NMR spectroscopy and X-ray powder diffraction.

Solid-state ^{13}C CP/MAS NMR spectra were obtained with ground crystals of the pure components and with crystals grown from various concentrations of the host and the guest. A section of the spectrum corresponding to the sp^2-hybridized carbon atoms is shown in Fig. 4. The spectrum corresponding to the pure crystalline ethyl-phenyl-containing salt **DB-EtPh-Pz** reveals signals with resonance frequencies that are analogous to those the pure acetophenone-containing salt **DB-AcPh-Pz**. A particularly diagnostic signal corresponding to the carbonyl group in **DB-AcPh-Pz**, shifts from at 196.8 ppm in crystals of the pure ketone to 193.2 ppm for crystals where ketone concentrations are only 5% and 10%. This difference indicates that ketone is in the crystal phase of **DB-EtPh-Pz**, rather than phase segregated into its own crystal phase. It is also significant that samples obtained with higher ketone concentration in solution displayed a carbonyl signal at the resonance frequency corresponding to the pure ketone phase, indicating that phase segregation had occurred. The fact that a mixture of mixed crystals and phase-segregated crystals was not obtained is a strong indication that growth occurs under kinetic control. Segregation of the two phases beyond the solubility limit was also observed by optical microscopy. While samples of **DB-EtPh-Pz** crystallized as fine needles with up to 10% **DB-AcPh-Pz**, samples set to crystallize with higher concentrations of the sensitizer resulted in the crystallization of the expected needles along with plates corresponding to **DB-AcPh-Pz** (*SI Appendix*, Fig. S2).[†]

Additional evidence for the formation of substitutional mixed crystals came by comparing X-ray powder diffraction patterns from samples obtained by mechanical grinding or by slow solvent evaporation with ketone concentrations of 5%, 8%, and 10% (*SI Appendix*, Fig. S54).

[†]Mixed crystal grown with **DB-EtPh-Pz** as a guest in **DB-AcPh-Pz** host showed a similar behavior with segregation occurring beyond the solubility limit (*SI Appendix*, Fig. S3).

A comparison of PXRD patterns corresponding to pure ketone-containing and ethylbenzene-containing crystals along with two-component samples grown from solution, and samples mechanically ground together display clear differences. While samples obtained by mechanical grinding display PXRD consistent with the sum of the two components those from samples grown from solution remained largely unchanged with some new peaks not originally present in the diffractograms of the pure components appearing at the point of saturation (*SI Appendix*, Fig. S54).

Nanocrystalline Suspensions. We have shown that spectroscopic measurements by transmission spectroscopic methods can be conveniently accomplished using suspensions of nanocrystalline particles of the same magnitude or smaller than the wavelength of the light used for excitation and detection (27), which in this case is in the range of 200 to 300 nm. Furthermore, high loading, optically dense nanocrystalline suspensions offer the opportunity to measure quantum yields of reaction in the solid state by making sure that all the photons from a calibrated light source are absorbed by the sample (28). Considering that quaternary ammonium salts of **DB-PhEt-Pz** and **DB-AcPh-Pz** are water soluble, we explored the formation of nanocrystalline suspensions of the pure components by precipitation from concentrated solutions of CH_2Cl_2 and CH_3OH (50:1) into vortexing hexane. Rapidly formed, milky white liquid samples were confirmed to be nanocrystalline suspensions by centrifugation and PXRD analyses of the recovered white powders. As shown in Fig. 5, diffractograms corresponding to the nanocrystalline suspension are essentially identical to those obtained from bulk crystalline specimens and to those obtained by simulation of the single crystal X-ray diffraction data. Dynamic light scattering measurements of freshly prepared suspensions revealed particles with a mean size of ca. 232 ± 106 nm (*SI Appendix*, Fig. S48). Attempts to prepare nanocrystalline suspension of mixed crystals by a similar procedure with solutions having varying amounts of the two components were not successful. However, we were able to obtain suspensions by a top–down approach suspending in hexane mixed crystals obtained by slow evaporation after thoroughly grounding them with a mortar and pestle.

Spectroscopic Characterization. The UV spectra of **DBs DB-AcPh-Pz** and **DB-EtPh-Pz** measured in 1.5×10^{-5} M acetonitrile are displayed in Fig. 6. Notably, the acetophenone chromophore in **DB-AcPh-Pz** (Fig. 6*A*, black line) has a strong absorption that extends from 265 to 360 nm. By contrast, samples of **DB-EtPh-Pz** (Fig. 6*A*, red line) have a much weaker absorption beyond

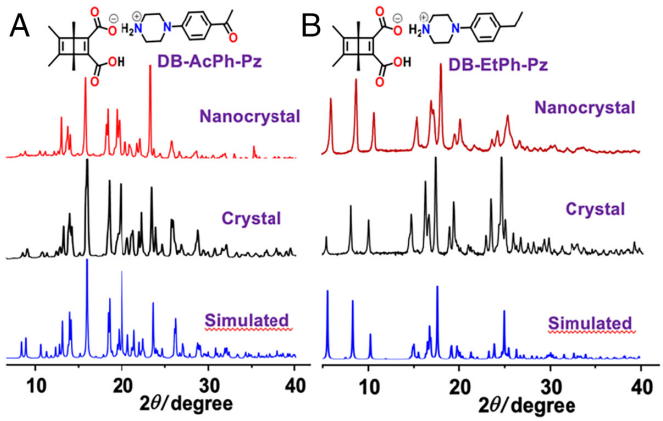

Fig. 5. Comparison of PXRD patterns, *Bottom* to *Top*, of (*A*) simulated, bulk crystals, and filtered nanocrystalline suspension of the ketone-containing **DB-AcPh-Pz**. (*B*) simulated, bulk crystal and nanocrystal from dried nanocrystalline suspension of crystal host **DB-EtPh-Pz**.

270 nm, such that selective excitation of the sensitizer is possible by taking advantage of the longer wavelengths. The absorption spectra of nanocrystalline suspensions of the ketone-containing **DB** reactant and benzene photoproduct illustrated in Fig. 6*B* display relatively minor changes in maximum absorption and linewidth. It is worth noting that the UV spectrum of the **DB** ion pair remained relatively unchanged in going from solution to the solid state. By contrast, the UV spectrum of the benzene ion pair blue shifted and became narrower in the solid state with a main peak and a shoulder (Fig. 6*B*). Based on this information, we carried out all photochemical experiments at l ≥ 340 nm, to selectively excite **DB-AcPh-PZ** both in pure samples and in mixed crystals.

To estimate the triplet energy of the 4-piperazinium-acetophenone chromophore, we obtained the phosphorescence spectrum of the acetophenone-containing benzene photoproduct, **HB-AcPh-Pz**. Excitation and emission measurements carried out in a dilute 2-methyltetrahydrofuran glass at 77 K are shown in Fig. 6*C*. The excitation spectrum shown in red cover the same region as its absorption spectrum at 300 K but is significantly more resolved. The emission spectrum extends from 400 to 600 nm with an envelope that displays λ_{max} at 422 and 449 nm that is consistent with a mixed n, π * and π, π * excited state (29). A triplet energy of ca. 69 kcal/mol can be determined from the onset of the lowest energy band.

Transient Absorption and Kinetics of the Quantum Chain Carrier in Solution. Laser flash photolysis experiments were performed with a Brilliant B Quantel Nd-YAG laser operating at 266 nm with a pulse width of ca. 8 ns as the excitation source. Samples were introduced to a mounted 1 cm quartz flow cell through a continuous one-pass flow system to ensure that only unreacted material was continuously sampled. Experiments were performed both in MeCN solution and with nanocrystals suspended in hexane. Samples were subject to 1 h of argon sparging and were continuously sparged throughout the experiment. To establish the triplet-triplet absorption and kinetics of the kinetic species potentially involved in the quantum chain we measured samples of the trifluoroacetic acid protonated form of the acetophenone-piperazine (**AcPh-PzH$^+$ CF$_3$CO$_2^-$**, Fig. 7*A*), and the quaternary ammonium salts of the reactant **DB** (**DB-AcPh-Pz**, Fig. 7*B*), and its benzene valence-bond isomer (**HB-AcPh-Pz**, Fig. 7*C*).

An acetonitrile solution of **AcPh-PzH$^+$ CF$_3$CO$_2^-$** obtained by protonation with trifluoroacetic acid (**CF$_3$CO$_2$H**) resulted in a transient band with a single l_{max} at 439 nm and a lifetime of 5.75 μs (Fig. 7*A*), which were quite different than those obtained from the corresponding free base (**AcPh-Pz**, *SI Appendix*, Fig. S55). As expected for a triplet excited state, the spectra can be readily quenched with dissolved oxygen. Measurements carried out with the two isomers of benzene (Fig. 7 *B* and *C*) revealed that their transient spectra are very different from those of their protonated triplet sensitizer (Fig. 7*A*). Based on precedent, these can be assigned to the substituted triplet benzene chromophore. The nearly identical spectra from **DB-AcPh-Pz** and **HB-AcPh-Pz** confirm the adiabatic nature of the triplet state reaction, as excitation of the **DB** results in the formation of the triplet benzene within ca. 8 ns laser pulse. Their triplet spectra are significantly narrower than that of **AcPh-PzH$^+$ TFA$^-$** with a λ_{max} at ca. 450 nm

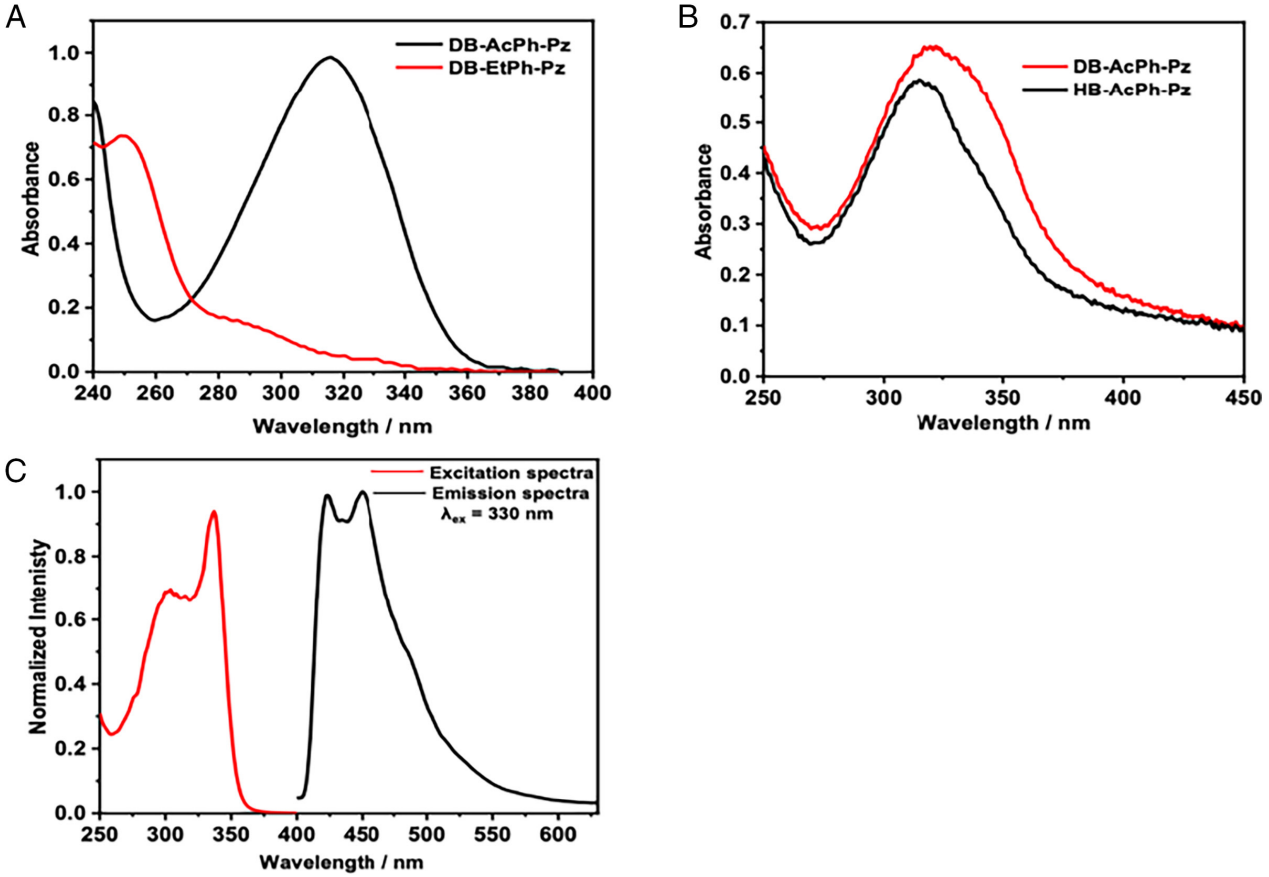

Fig. 6. (*A*) Comparison of UV-vis spectra from 1.5 × 10^{-5} M MeCN solutions of **DB-AcPh-Pz** (black line), 1.5 × 10^{-5} (M) **DB-AcPh-Pz** (red line). (*B*) Comparison UV-vis spectra of **DB-AcPh-Pz** (red line), **HB-AcPh-Pz** (black line), in nanocrystalline suspension. (*C*) Normalized Phosphorescence excitation (red line) and emission (black line) spectra of **HB-AcPh-Pz** in 2-methyltetrahydrofuran glass at 77 K. The emission spectrum was obtained by excitation at 330 nm and the excitation spectrum by detection at 450 nm.

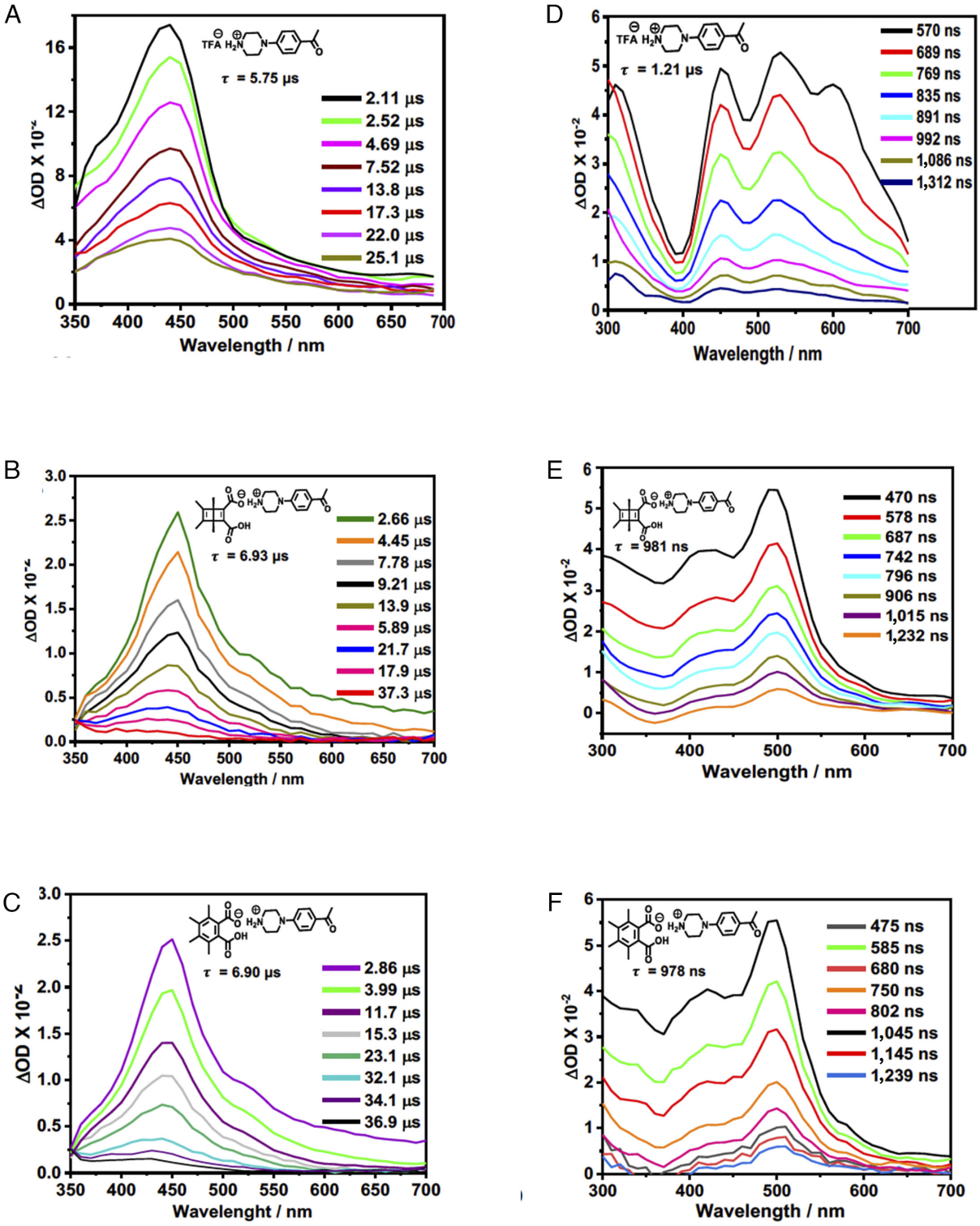

Fig. 7. Transient absorption spectra of (*A*) 2.2 mM $[AcPh\text{-}Pz\text{-}H]^+$ with lifetime (τ = 5.75 µs), (*B*) 1.6 mM DB-AcPh-Pz with lifetime (τ = 6.93 µs) (*C*) 1.6 mM HB-AcPh-Pz with lifetime (τ = 6.90 µs), acquired immediately after the laser pulse in Ar saturated MeCN. Transient absorption spectra of (*D*) 4.6 mM $[AcPh\text{-}Pz\text{-}H]^+$ with lifetime (τ = 1.21 µs), (*E*) 5.7 mM DB-AcPh-Pz with lifetime (τ = 981 ns), (*F*) 5.7 mM HB-AcPh-Pz with lifetime (τ = 978 ns) acquired immediately after the laser pulse in nanocrystalline suspension.

and a shoulder at ca. 525 nm. The triplet decays measured in the range of 350 to 700 nm were fit to monoexponential functions with lifetimes of 6.93 µs and 6.90 µs, respectively, for samples of **DB-AcPh-Pz** and **HB-AcPh-Pz**, strongly supporting the identity of the two transients.

Transient Absorption and Kinetics of the Quantum Chain Carrier in Crystals. Samples of the protonated amine sensitizer **AcPh-PzH$^+$TFA$^-$** suspended in hexane exhibited a transient spectrum quite different from the one recorded in solution, with a broad band displaying three maxima at λ_{max} = 460 nm, 540 nm, and

612 nm (Fig. 7*D*) and a monoexponential lifetime of 1.2 μs. We confirmed that the solid-state reaction is also adiabatic as the spectrum obtained from nanocrystals of **DB-AcPh-Pz** (Fig. 7*E*) is essentially identical to the one from **HB-AcPh-Pz** (Fig. 7*F*), and they are both quite distinct from that of the triplet sensitizer. Their spectra exhibit a band extending from ca. 350 nm to 600 nm with one maximum at 410 nm and a second one about 20% more intense at 500 nm (Fig. 7 *E* and *F*). The two decays were also similar to each other and were fit to monoexponential functions with time constants of 981 ns and 978 ns in the range from 350 to 700 nm. In order to confirm the sensitized nature of the observed transients we also conducted experiments with nanocrystalline suspensions of Dewar benzene diacid **DB-CO_2H** and **DB** ion pair **DB-EtPh-Pz**, and both failed to produce an observable transient on their own, as expected for a fast nonadiabatic singlet state reaction and a very inefficient intersystem crossing.

Quantum Chain Reaction in Crystalline Suspensions. The first sign of a quantum chain reaction is the formation of a large amount of product after a relatively brief exposure to light. Quantum yield measurements in solution were conducted in triplicate with deoxygenated samples of **DB**s **DB-AcPh-Pz** and **DB-EtPh-Pz** in 15 mM DMSO-d_6 using λ ≥ 340 nm in 3 mL Pyrex tubes for only 15 s irradiation in Hanovia. While samples of **DB-EtPh-Pz** gave conversion values of ca. 5 ± 1%, the triplet-sensitized **DB DB-AcPh-Pz** resulted in ca. 51 ± 2% conversion. We also showed that reaction in the case of **DB-EtPh-Pz** is concentration independent, and that its quantum yield of reaction in solution is F ≈ 1. By contrast, the quantum yield of reaction for the triplet-sensitized **DB DB-AcPh-Pz** in 15 mM DMSO was estimated to be ca. Φ = 5.2 ± 0.7. The quantum efficiency of the free Dewar benzene diacid **DBDA** in 15 M DMSO upon the addition of between 0.1% and 10% of the ketone-containing ion pair **DB-AcPh-Pz** resulted in the expected increase in quantum yield from Φ = 1.2 to 3.2 which, while modest, highlights the important role of a triplet state to prolong the chain.

Since we were unable to obtain nanocrystalline suspensions of mixed crystals under precipitation conditions in hexane, we opted for a top–down approach for experiments involving pure **DB-AcPh-Pz**, **DB-EtPh-Pz**, and mixed crystals with **DB-AcPh-Pz** loading from 0.1 to 10%. We noticed that photochemical reactions carried out under identical conditions with microcrystalline suspensions of **DB-EtPh-Pz** and **DB-AcPh-Pz** resulted in conversion values of 4 ± 1% and 81 ± 2%, respectively, after a 15 min irradiation time. The trailing absorption at λ = 340 nm (Fig. 6*A*) is responsible for the small conversion in the case of **DB-EtPh-Pz**. By contrast, mixed crystalline suspension of **DB-EtPh-Pz** with 0.1% **DB-AcPh-Pz** resulted in 91 ± 2% conversion in the same amount of time. Considering that triplet quantum chain reactions in nanocrystalline suspensions are expected to have quantum yields that are one to three orders of magnitude greater than those observed in solution, the use of conventional chemical actinometers is not practical, as one would have to quantify vastly different conversion values. To mitigate this problem, we recently took advantage of 1% or 2% transmission filters to attenuate the light going to the quantum chain reaction, such that the moles of product formed from a normal actinometer and from the quantum chain reaction would be similar, despite having received very different (but measurable) number of photons. We established that the quantum yield of reaction of microcrystalline suspensions of benzophenone-sensitized **DB DB-CO_2BPh** (Fig. 1*F*) prepared by a top–down method has a value of Φ ≈ 300 ± 10 (19) and we decided to use it as a secondary actinometer for this study.

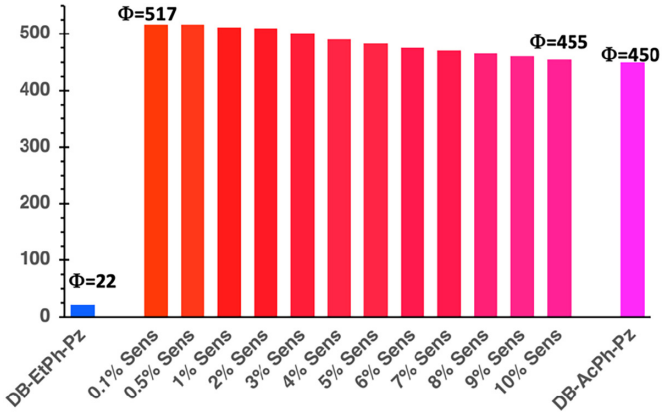

Fig. 8. Quantum yield of formation of **HB-EtPh-Pz** in pure crystals of **DB-EtPh-Pz** (blue bar) and **DB-AcPh-Pz** (magenta bar), and mixed crystals of **DB-EtPh-Pz** with 0.1 to 10% incorporated **DB-AcPh-Pz** (red bars).

As shown in Fig. 8, quantum yields were measured with suspensions of pure **DB-AcPh-Pz** and **DB-EtPh-Pz**, as well as with mixed crystals of **DB-EtPh-Pz** containing between 0.1% and 10% **DB-AcPh-Pz**. The results revealed that quantum yield of product formation from self-triplet-sensitized **DB-AcPh-Pz** is ca. Φ = 450, while the one from **DB DB-EtPh-Pz** with no triplet sensitizer was estimated to be ca. Φ = 22 ± 2, reflecting a significantly shorted quantum chain length. The effect of added sensitizer within the 0.1 to 10% solubility limits of the two component crystals revealed a more efficient reaction when the concentration of the sensitizer is lower. A maximum quantum yield of Φ = 517 with 0.1% sensitizer steadily decreased to Φ = 455 when the sensitizer reached a 10% value. Samples of **DB-EtPh-Pz** crystallized with less than 0.1%, or more than ca. 20% **DB-AcPh-Pz** failed to form mixed crystals and their quantum yields reverted to those of the pure **DB-EtPh-Pz** phase, i.e., Φ = 22. It should be noted that random errors in Fig. 8 are relatively small, oscillating between 2% and 10%. While systematic errors arising from the assumed quantum yield of the actinometer, determinations of light absorption, analytical determinations, and others, cannot be discounted, comparison across samples unambiguously established the key role of the triplet sensitizer and efficient triplet exciton delocalization in the crystalline state. The lack of a quantum chain when sensitizer values are outside the 0.1 to 10% concentration window highlights the strict solubility limits of the two-component mixed crystal. An increase in the quantum yield of the chain reaction as the concentration of the triplet sensitizer decreases is consistent with a self-quenching mechanism between nearby ketone chromophores. However, to the extent that results from different crystal lattices may be compared, a modest 12% decrease from Φ = 517 to Φ = 450 when the ketone concentration changes from 0.1 to 100%, suggests that self-quenching plays a minor role with the acetophenone-piperazinium ion pairs. Furthermore, considering a quantum yield Φ = 450 and a triplet benzene chain carrier lifetime of 980 ns in suspensions of **DB-AcPh-Pz**, one can estimate an average of ca. 2.2 reaction per nanosecond, a relatively long-time constant that is likely determined by the adiabatic reaction.

Conclusions

The design of tailor-made mixed crystals based on the use of ionic auxiliaries as crystal engineering tools and reaction components is demonstrated in the exciton-enabled, triplet-sensitized quantum chain reaction of **DB** diacid monosalts. Strong evidence was obtained

for the triplet sensitizer, a triplet state adiabatic reaction, and triplet exciton delocalization as essential elements for a photochemical reaction that generates over 500 reaction events per photon absorbed. To demonstrate these results, we used a design based on crystals of hexamethyl-Dewar benzene-1,2-diacid monosalts equipped with N-(4-ethylphenyl)- and N-(4-acetophenyl)-linked piperazinium cations, **DB-EtPh-Pz** and **DB-AcPh-Pz** respectively, crystal former and triplet sensitizer. Despite having nearly identical ion-pair structures, hydrogen bonding motifs, and space groups (C2/c), crystals of **DB-EtPh-Pz** and **DB-AcPh-Pz** present substantially different packing motifs, which limit the solubility of one component in the crystal lattice of the other. Product analysis of **DB**s **DB-EtPh-Pz** and **DB-AcPh-Pz** in solution and in the solid state revealed a very clean valence-bond isomerization reaction to the corresponding benzenes, **HB-EtPh-Pz** and **HB-AcPh-Pz**, respectively. Transient spectroscopy in solution and in crystalline suspensions confirmed the adiabatic nature of the reaction, as the spectrum and lifetime from triplet-sensitized **DB** were nearly identical as those obtained from the corresponding triplet-sensitized spectrum of the benzene photoproduct. Pure components of **DB-EtPh-Pz** and **DB-AcPh-Pz**, and mixed crystals containing between 0.1% and 10% of the latter triplet sensitizer were characterized by PXRD, ^{13}C CPMAS NMR, and thermal analysis. Quantum yield determinations in the solid state for pure crystals of **DB-EtPh-Pz** and **DB-AcPh-Pz** revealed vastly different values of Φ = 22 and Φ = 450, respectively, while mixed crystals of **DB-EtPh-Pz** with varying amounts of **DB-AcPh-Pz** gave quantum yield that varied from Φ = 517 to Φ = 450 as the sensitizer concentration varied from 0.1 to 10%. Taking the quantum yield of reaction and the lifetime of the triplet carrier we can conclude an operating mechanism that includes as many as ca. 500 steps per photon absorbed with as many as ca. 2.2 reactions per nanosecond. Considering that triplet energy transfer in the solid state is likely to occur in the picosecond time regime, longer quantum chains will require faster triplet state adiabatic reactions and longer-live carriers. One may expect that photochemical reactions that significantly amplify the number of photons absorbed will be found interesting in analytical chemistry, materials applications, and the life sciences.

Data, Materials, and Software Availability. All study data are included in the article and/or *SI Appendix*.

ACKNOWLEDGMENTS. We are grateful to the NSF for support of this work through grant CHE-2154210.

1. A. Rao, R. H. Friend, Harnessing singlet exciton fission to break the Shockley-Queisser limit. *Nat. Rev. Mat.* **2**, 17063 (2017).
2. D. N. Congreve *et al.*, External quantum efficiency above 100% in a singlet-exciton-fission–based organic photovoltaic cell. *Science* **340**, 334–337 (2013).
3. R. R. Islangulov, J. Lott, C. Weder, F. N. Castellano, Noncoherent low-power upconversion in solid polymer films. *J. Am. Chem. Soc.* **129**, 12652–12653 (2007).
4. P. Bharmoria, H. Bildirir, K. Moth-Poulsen, Triplet–triplet annihilation based near infrared to visible molecular photon upconversion. *Chem. Soc. Rev.* **49**, 6529–6554 (2020).
5. G. Kuzmanich *et al.*, Solid-state photodecarbonylation of diphenylcyclopropenone: A singlet state quantum chain reaction made possible by ultrafast energy transfer. *J. Am. Chem. Soc.* **130**, 1140–1141 (2008).
6. J. G. Gillmore *et al.*, Quantum amplified isomerization: A new concept for polymeric optical materials. *Macromolcules* **38**, 7684–7694 (2005).
7. The first documented quantum chain reaction involves the triplet sensitized photoisomerization of 2,4-hexadiene: H. L. Hyndman, B. M. Monroe, G. S. Hammond, Mechanisms of photochemical reactions in solution. LX. Photochemical isomerization of 2,4-hexadiene via a quantum-chain mechanism. *J. Am. Chem. Soc.* 91, 2852–2859 (1969).
8. J. Saltiel, D. E. Townsend, A. Skyes, Quantum chain process in the sensitized cis-trans photoisomerization of 1,3-dienes. *J. Am. Chem. Soc.* **95**, 5968–5973 (1973).
9. H. Möllerstedt, O. Wennerström, Catalysis of a photochemical quantum chain process: Optimal conditions for catalyzed quantum chain *cis–trans* photoisomerizations of a styrylpyrene. *J. Photochem. Photobiol. A* **139**, 37–43 (2001).
10. N. J. Turro, W. H. Waddell, Quantum chain processes. Direct observation of high quantum yields in the direct and photosensitized excitation of tetramethyl-1,2-dioxetane. *Tetrahedron Lett.* **25**, 2069–2072 (1975).
11. V. P. Kazakov, A. I. Voloshin, N. M. Shavaleev, Chemiluminescence in visible and infrared spectral regions and quantum chain reactions upon thermal and photochemical decomposition of adamantylideneadamantane-1,2-dioxetane in the presence of chelates $Pr(dpm)_3$ and $Pr(fod)_3$. *J. Photochem. Photobiol. A* **119**, 177–186 (1998).
12. N. J. Turro, V. Ramamurthy, T. H. J. Katz, Energy storage and release direct and sensitized photoreactions of Dewar benzene and prismane. *Nouv. J. Chim.* **1**, 363 (1977).
13. S. Takeuchi, T. Tahara, Femtosecond absorption study of photodissociation of diphenylcyclopropenone in solution: Reaction dynamics and coherent nuclear motion. *J. Chem. Phys.* **120**, 4768–4776 (2004).
14. G. Kuzmanich, M. N. Gard, M. A. Garcia-Garibay, Photonic amplification by a singlet-state quantum chain reaction in the photodecarbonylation of crystalline diarylcyclopropenones. *J. Am. Chem. Soc.* **131**, 11606–11614 (2009).
15. S. C. Doan, G. Kuzmanich, M. N. Gard, M. A. Garcia-Garibay, B. J. Schwartz, Ultrafast spectroscopic observation of a quantum chain reaction: The photodecarbonylation of nanocrystalline diphenylcyclopropenone. *J. Phys. Chem. Lett.* **3**, 81–86 (2012).
16. J. K. Crandall, C. F. Mayer, Benzene-photosensitized transformations of the four geometrical isomers of 1,5,9-cyclododecatriene. *J. Am. Chem. Soc.* **89**, 4374–4380 (1967).
17. R. R. Hentz, R. M. Thibault, Concentration and temperature dependence of th quantum yield and lifetime of the lowest triplet state of benzene in the liquid phase. *J. Phys. Chem.* **77**, 1105–1111 (1973).
18. J. T. Dubois, F. Wilkinson, Triplet state of benzene. *J. Chem. Phys.* **3**, 2541–2547 (1963).
19. For a report of a triplet chain reaction of Dewar benzene diesters in polymers please see: L. Ferrar *et al.*, Quantum amplified isomerization in polymers based on triplet chain reactions. *J. Org. Chem.* **73**, 5683–5692 (2008).
20. E. Rivera, I. Paul, J. Fajardo Jr., M. A. Garcia-Garibay, Quantum chain amplification in nanocrystalline Dewar benzenes by intramolecular sensitization. *Chem. Sci.* **14**, 5802–5810 (2023)
21. A. I. Kitaigorodski, *Mixed Crystals* (Springer Verlag, Berlin, 1984).
22. M. A. Oliveira, M. L. Peterson, D. Klein, Continuously substituted solid solutions of organic co-crystals. *Cryst. Growth Des.* **8**, 4487–4493 (2008).
23. Y. Zhen *et al.*, Organic solid solution composed of two structurally similar porphyrins for organic solar cells. *J. Am. Chem. Soc.* **137**, 2247–2252 (2015).
24. M. A. Lusi, Rough guide to molecular solid solutions: Design, synthesis and characterization of mixed crystals. *CrystEngComm* **20**, 7042–7052 (2018).
25. J. N. Gamlin *et al.*, The ionic auxiliary concept in solid state organic photochemistry. *Acc. Chem. Res.* **29**, 203–209 (1996).
26. J. B. Koster, G. J. Timmermans, H. Van Bekkum, Reaction of the tetramethylcyclobutadiene-aluminum chloride complex with dienophilic esters. *Synthesis* **3**, 139–140 (1971).
27. K. K. Chin *et al.*, Organic molecular nanocrystals: Triplet–triplet absorption, phosphorescence, and circular dichroism of chiral crystals of benzophenone. *Chem. Commun.* **41**, 4266–4268 (2007).
28. M. Veerman, M. J. E. Resendiz, M. A. Garcia-Garibay, Large-scale photochemical reactions of nanocrystalline suspensions: A promising green chemistry method. *Org. Lett.* **8**, 2615–2617 (2006).
29. S. Yabumoto, S. Shigeto, Y.-P. Lee, H. Hamaguchi, Ordering, interaction, and reactivity of the low-lying n, π^* and π . π^* excited triplet states of acetophenone derivatives. *Angew. Chem. Int. Ed.* **49**, 9201–9205 (2010).